Quasi-TEM Analysis of Microwave Transmission Lines by the Finite-Element Method

ZORICA PANTIĆ AND RAJ MITTRA, FELLOW, IEEE

Abstract —**This paper describes a finite-element approach to the quasi-TEM analysis of several different types of isolated and coupled microwave transmission lines. Both the first- and higher order ordinary elements, as well as singular and infinite elements, are used to solve for the potential and field distributions in the cross section of the line. Next, the cross-sectional field distribution is inserted in a variational expression to compute the capacitance per unit length of the line, and the effective permittivity and characteristic impedance of the line are obtained from the capacitance value. A perturbational approach is developed for estimating the losses due to conductor and dielectric dissipation and computing the attenuation constant. Both the upper and lower bounds for the capacitance and the characteristic impedance are found by solving the original and the corresponding dual problem.**

Lines treatable by this method may contain an arbitrary number of arbitrarily shaped conductors, including a system of conductors placed either above a single ground plane or between two parallel ground planes, and inhomogeneous dielectric regions that can be approximated locally by a number of homogeneous subregions.

The results obtained using the finite-element procedure have been compared for various types of microwave transmission lines and have been found to agree well with available theoretical and measured data.

I. Introduction

THE ACCURATE PREDICTION of the characteristic impedance, attenuation, coupling, crosstalk, etc., in microstrips, striplines, and similar transmission lines is important in microwave and millimeter-wave integrated circuits, digital circuit design, communication, and other applications. The objective of this paper is to consider microwave transmission lines with rather arbitrary configuration and to present a computer-aided analysis that allows simple and accurate calculation of its design parameters.

In the past, microwave transmission lines have been thoroughly investigated by many authors and many approaches to analyzing them have been devised, e.g., the Green's function techniques [1]–[6], conformal mapping [7]–[9], variational methods [10], [11], Fourier transform method [12], [13], Fourier integral method [14], spectral-domain method [15]–[17], boundary element method [18], [19], and finite-element method [20]. All of the above methods, with the exception of the last two are restricted in their application to transmission lines in which the conductors are thin strips and/or the dielectrics' inserts have planar interfaces. In contrast, the finite-element method (FEM) is capable of handling transmission lines with rather arbitrary configurations, since the lines treatable by this method may contain an arbitrary number of conductors of arbitrary shape and inhomogeneous dielectric regions that can be approximated locally by a number of homogeneous subregions. Because of its generality, the FEM is employed in this paper for the analysis of several representative microwave transmission lines of practical interest. The analysis is based on a quasi-TEM model which is often adequate for microwave frequencies in communication applications and for typical pulse rise times of interest in high-speed digital circuit design.

Both the first- and higher order ordinary elements, as well as singular and infinite elements, are used in the FEM algorithm to solve for the quasi-static potential and the corresponding field distribution in a microwave transmission line. The capacitance per unit length of the line is obtained from a variational expression, and the effective dielectric permittivity, characteristic impedance, and phase velocity are also calculated. The upper and lower bounds of the capacitance and the characteristic impedance are derived by solving both the original and the dual problem. Finally, a perturbation method is used to compute the losses due to both the conductor and dielectric dissipations.

The characteristic impedance and loss characteristics have been calculated for various transmission lines of interest and very good agreement with available theoretical and experimental data has been obtained.

II. Finite-Element Model of a Microwave Transmission Line

Consider a microwave transmission line with an arbitrary cross section consisting of a number of arbitrarily shaped conductors and inhomogeneous dielectric regions which can be approximated locally by homogeneous subregions (Fig. 1). Let us assume that the line is uniform along its longitudinal (z) axis and let ϵ and μ ($=\mu_0$) denote the

Manuscript received January 3, 1986; revised May 28, 1986. This work was supported in part by the Army Research Office under Contract No. DAAG 29-85-K-0183, by the Office of Naval Research under Contract No. N00014-85-K-0619, and by the Joint Services Electronics Program under Contract No. N00014-84-C-0149.

Z. Pantic is a Visiting Research Associate at the University of Illinois, on leave from the University of Niš, Niš, Yugoslavia.

R. Mittra is with the Electrical and Computer Engineering Department, University of Illinois, Urbana.

IEEE Log Number 8610509.

0018-9480/86/1100-1096$01.00 ©1986 IEEE

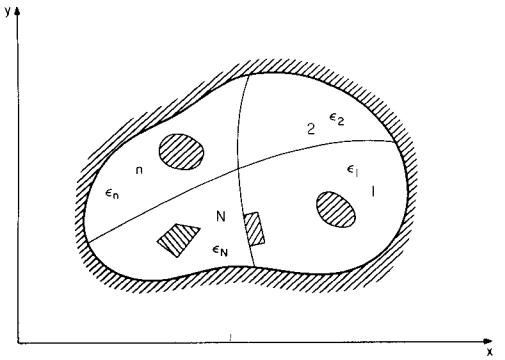

Fig. 1. Cross section of a microwave transmission line.

permittivity and permeability, respectively, of the medium in each homogeneous subregion.

We assume a quasi-TEM model, i.e., that the dominant mode propagating along the line is a TEM mode. Under this approximation, the problem is reduced to that of finding the scalar potential function ϕ satisfying the Poisson's equation

$$\Delta\phi = -\frac{\rho}{\epsilon} \tag{1}$$

subject to the (appropriate) boundary conditions

$$\phi = \phi_0 \text{ on } \Gamma_1, \frac{\partial\phi}{\partial n} = 0 \text{ on } \Gamma_2 \tag{1a}$$

where ρ is the volume charge distribution, ϵ is the dielectric permittivity, and Γ_1 and Γ_2 are complementary portions of the boundary Γ of the domain S in which (1) is defined.

In order to apply the finite-element approach to the problem at hand, we formulate it in variational terms. The correct solution of (1) is one that minimizes the energy functional

$$F = \frac{1}{2}\int_S \epsilon|\nabla\phi|^2\, dS - \int_S \rho\phi\, dS. \tag{2}$$

Equation (1) is the Euler equation of the functional F [27] satisfying the essential boundary condition of the Dirichlet type, viz.,

$$\phi = \phi_0 \text{ on } \Gamma_1 \tag{2a}$$

and the natural boundary condition of the Neuman type, i.e.,

$$\frac{\partial\phi}{\partial n} = 0 \text{ on } \Gamma_2. \tag{2b}$$

According to the FEM procedure, the cross section of the line, domain S, is subdivided into finite elements in an arbitrary manner provided that all the dielectric interfaces coincide with the element sides. Although a variety of different elements can be chosen, the triangular first- or higher order [21] elements are adopted in this study. It has been shown [21] that the accuracy and efficiency of computation can be substantially enhanced via the use of the high-order elements compared with the case where only the first-order elements are employed if the same number of nodes is used. On the other hand, a large number of simple elements are clearly advantageous where a complicated boundary shape needs to be modeled.

However, when there are field singularities caused by edges in the cross section of the line, a very fine mesh of first- or high-order elements is required to obtain an accurate solution. However, in order to improve accuracy and reduce the number of necessary nodes, singular elements [22] are used in this study. A singular element with labeled nodes and associated triangular polar coordinate system (ρ, σ) is shown in Fig. 2.

The global Cartesian coordinates are then

$$\begin{aligned} x &= x_1 + \rho[(x_2 - x_1) + \sigma(x_3 - x_2)] \\ y &= y_1 + \rho[(y_2 - y_1) + \sigma(y_3 - y_2)]. \end{aligned} \tag{3a}$$

The scalar potential distribution function that takes into account the field singularity at the node 1 ($\rho = 0$) has the following form:

$$\phi = \Phi_1(1-\rho^\lambda) + \Phi_2\rho^\lambda(1-\sigma) + \Phi_3\rho^\lambda\sigma, \qquad \frac{1}{2} < \lambda < 1 \tag{3b}$$

where coefficient λ is chosen in accordance with the Meixner edge condition [23], and Φ_1, Φ_2, Φ_3 are corresponding nodal potentials. The linear variation of the scalar potential along the side 2–3 is provided so that the element is compatible with first-order ordinary elements.

Although open-type transmission lines can be treated by the conventional finite-element method with the shielding far away from the region of interest, the computation efficiency can be substantially improved if infinite elements [24] are used. Consider first the line consisting of a number of conductors arbitrarily placed between two parallel ground planes (Fig. 3(a)).

The entire domain can be divided into the near-field region (n.f.), which is the region of interest, and the far-field region (f.f.), which is unbounded. They have a common boundary, referred to as the far-field boundary (f.f.b.). The n.f. region is then divided into finite triangular elements in the usual manner, while the f.f. region is divided into infinite elements. Each infinite element has two common nodes (lying on the f.f.b.) with an ordinary first-order element and two sides parallel to the x axis.

Consider the infinite element with nodes 1 and 2 (Fig. 3(b)) and introduce normalized coordinates

$$\xi = \frac{x}{x_1}, \eta = \frac{y - y_1}{y_2 - y_1}, \qquad x_1 < x < \infty, y_1 \leqslant y \leqslant y_2. \tag{4a}$$

Because of the presence of ground planes, the far field of the system is equivalently a dipole field. For such a dipole with translational symmetry, whose moment $\vec{p}$ is oriented along y axes, the scalar potential function in the cylindrical coordinate system (r, θ) has the form

$$\phi_D = \frac{p}{2\pi\epsilon}\frac{\sin\theta}{r}. \tag{4b}$$

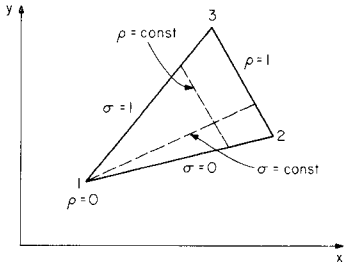

Fig. 2. Singular element.

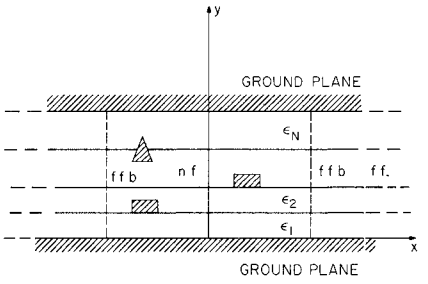

(a)

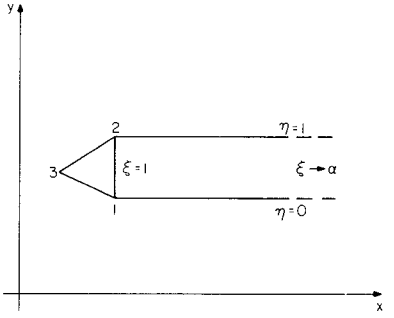

(b)

Fig. 3. (a) Line consisting of a system of conductors placed between two ground planes (n.f.: near field; f.f.: far field; f.f.b.: far-field boundary). (b) Infinite element type I.

Written in the x, y system, ϕ_D is given by

$$\phi_D = \frac{p}{2\pi\epsilon}\frac{y}{x^2}. \tag{4c}$$

Thus, in the normalized coordinates ξ, η the potential function ϕ can be written in terms of the nodal potentials Φ_1, and Φ_2 as

$$\phi = \frac{1}{\xi^2}\left[\Phi_1(1-\eta) + \Phi_2\eta\right]. \tag{4d}$$

The next type of open region problem involves a system of conductors above a ground plane. The procedure is similar to that in the previous case. The entire domain is divided into n.f. and f.f. regions (Fig. 4(a)). The n.f. region is divided into the usual triangular mesh and the f.f. region is divided into infinite elements of two different types, I and II. The infinite element type I is the element previously discussed. Consider now the infinite element of type II with nodes 1, 2 and radial sides intersecting at point (x_0, y_0) (Fig. 4(b)) and introduce triangular polar coordi-

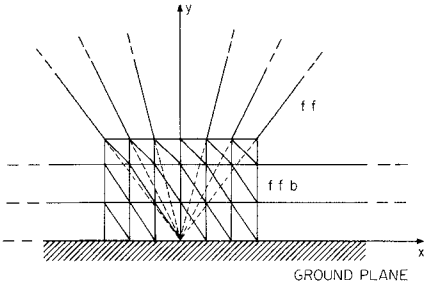

(a)

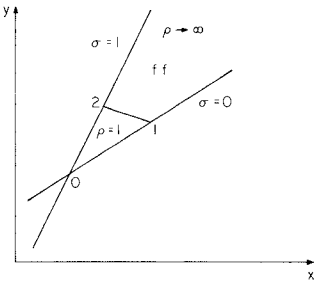

(b)

Fig. 4. (a) Line consisting of a system of conductors placed above ground plane. (b) Infinite element type II.

nates ρ, σ, which are related to the global Cartesian coordinates by the relations

$$\begin{aligned} x &= x_0 + \rho\left[(x_1 - x_0) + \sigma(x_2 - x_1)\right] \\ y &= y_0 = \rho\left[(y_1 - y_0) + \sigma(y_2 - y_1)\right]. \end{aligned} \tag{5a}$$

The scalar potential distribution within the element is approximated by

$$\phi = \frac{1}{\rho}\left[\Phi_1(1-\sigma) + \Phi_2\sigma\right] \tag{5b}$$

where Φ_1, Φ_2 are nodal potentials.

For both types of infinite elements, the linear variation of the potential function along the side 1–2 (common side with a corresponding ordinary element) is provided. These elements are compatible with ordinary first-order elements and satisfy completeness, finiteness, and radiation conditions [24].

Once the potential distribution is known, the capacitance per unit length C is readily obtained from the variational expression

$$C = \frac{2W}{V^2} \tag{6a}$$

where W is the energy per unit length of the line and V is the conductor potential. The upper and lower bounds of the capacitance are found by solving the original and dual problem [25].

The effective (dielectric) permittivity is

$$\epsilon_{\text{eff}} = \frac{C}{C_0} \tag{6b}$$

where C is the capacitance of the actual line and C_0 is the free-space capacitance of the line. The phase velocity is

$$v_\phi = \frac{c}{\sqrt{\epsilon_{\text{eff}}}} \tag{6c}$$

where c is the velocity of light in free space. The characteristic impedance is

$$Z_c = \frac{1}{v_\phi C}. \tag{6d}$$

The expressions given in (6a)–(6d) are for a single line, but the same procedure can be applied to find the capacitance and characteristic impedance for even and odd modes of two coupled lines or to find capacitance and impedance matrices for a system of n lines. The electromagnetic field distribution can also be obtained

$$\vec{E}_0 = -\nabla\phi, \vec{H}_0 = -\frac{1}{\eta}\vec{E}_0 \times \hat{z} \tag{7a}$$

where $\hat{z}$ is unit vector in the z direction and η is the intrinsic impedance of the medium

$$\eta = (\mu_0/\epsilon_0\epsilon_{\text{eff}})^{1/2}. \tag{7b}$$

Next, we employ a perturbational approach to solve for the attenuation constants due to dielectric and conductor losses

$$\alpha_d = \frac{P_d}{2P_0}, \alpha_c = \frac{P_c}{2P_0} \tag{8a}$$

where P_0 is the time-averaged power flow along the line, and P_d and P_c are the time-averaged powers dissipated in the dielectrics and conductors, respectively.

Dielectric losses are calculated using the formula

$$P_d = \omega\epsilon \tan\delta \int_{S_{\text{diel}}} |\vec{E}_0|^2 \, dS \tag{8b}$$

where the loss tangent $\tan\delta$ is assumed to be sufficiently small so that the perturbed fields can be approximated by the fields for the lossless condition $\vec{E}_0, \vec{H}_0$; $\omega = 2\pi f$ is the angular frequency; and S_{diel} is the area of cross section covered by the dielectric.

Losses due to the imperfect conductors are obtained via the conventional perturbation formula [26]

$$P_c = R_s \int_C |\vec{H}_0|^2_{\text{tang}} \, dl \tag{8c}$$

where R_s is the surface resistance and $|\vec{H}_0|_{\text{tang}}$ is the magnitude of the tangential magnetic field at the conducting surfaces (line C) for the lossless case.

The average power propagating along the line is given by

$$P_0 = \text{Re} \int_S (\vec{E}_0 \times \vec{H}_0^*) \cdot \hat{z} \, dS \tag{8d}$$

where S is the complete cross section of the line.

For the conductor loss calculation, special finite-element matrices have been derived [27]. Consider a high-order element where vertices are labeled as nodes i, j, k (Fig. 5). Suppose that the side $j-k$ is an imperfect conductor of surface resistance R_s. Then the losses in that side can be expressed as

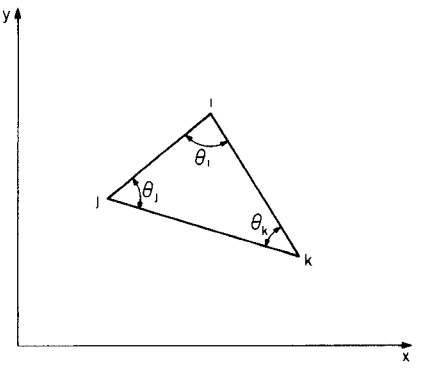

Fig. 5. Ordinary triangular element.

$$P_c^i = \frac{R_s}{\eta^2}\left[P_i \cot\theta_i + P_j \cot\theta_j + P_k \cot\theta_k\right][\Phi]$$

where $[\Phi]$ is a column vector of nodal potentials for the element; $\theta_i, \theta_j, \theta_k$ are the included angles at vertices i, j, k, respectively; and P_i, P_j, P_k are matrices of the numerical coefficients which do not depend on the triangle shape.

III. Numerical and Experimental Results

On the basis of described finite-element procedures, two different computer software packages have been developed for solving the problem at hand. The first of these is employed for semiautomatic mesh generation of first- or high-order ordinary elements, including singular and infinite elements if necessary. The second package calculates the potential and field distributions, capacitance per unit length, characteristic impedance, effective permittivity, and attenuation due to conductor and dielectric losses. The linear system of equations derived from the application of the FEM method is rather sparse and special techniques for the solution of such equations can be employed to achieve enhanced computational efficiency. Two such techniques are the direct envelope method and the band method with node reordering. These are useful for smaller problems with a few hundred nodes. For large systems of equations (a few thousand nodes), the conjugate gradient method is suggested because it requires the storage of only nonzero elements. Preconditioning is accomplished via incomplete Cholesky decomposition [28], which leads to the acceleration of the iteration procedure.

To demonstrate the quality and the accuracy of the finite-element-method analysis of the previous section, the solutions for sample problems are given and are compared with available theoretical and experimental data, as well as with measured results.

The first example considered is the problem of a shielded, multilayered, thick strip transmission line, shown in Fig. 6. The corresponding triangular mesh for one-half of the line is presented in Fig. 7. The characteristic impedance of the line is calculated for a few different thicknesses of the

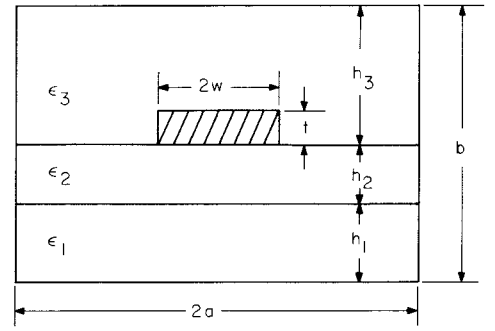

Fig. 6. Thick-strip transmission line with multidielectric layers and shielding structure ($h_1 = h_3 = 0.4b$; $h_2 = 0.2b$; $2w = 0.5b$; $\epsilon_1 = \epsilon_3 = \epsilon_0$; $\epsilon_2 = 9.35\epsilon_0$).

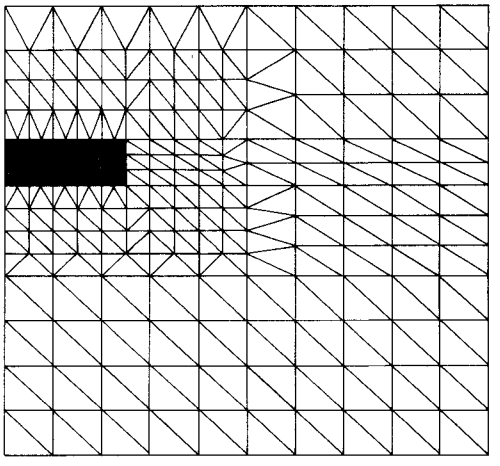

Fig. 7. Triangular mesh for thick-strip transmission line with 208 nodes and 351 elements.

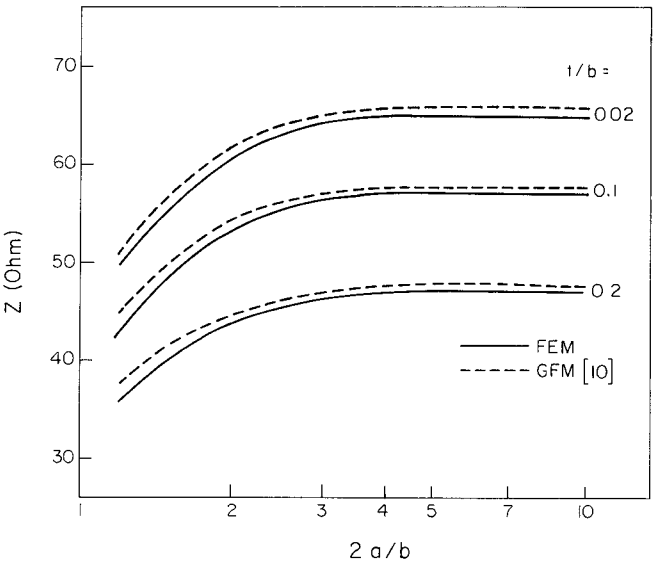

Fig. 8. Characteristic impedance Z of thick-strip transmission line.

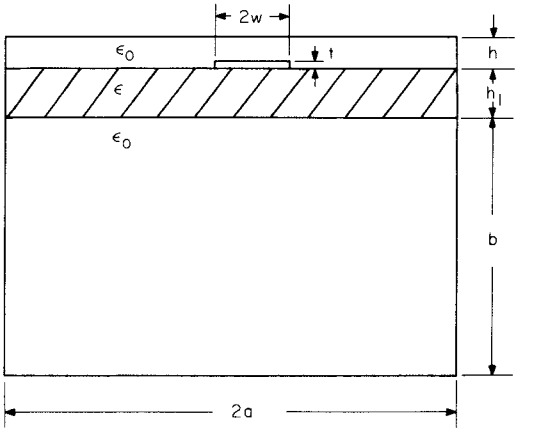

Fig. 9. Generic cross section of inverted microstrip with shielding structure ($h = 0.381$ mm; $h_1 = 0.508$ mm; $t = 0$; $2a = 10$ mm; $b = 10$ mm; $\epsilon = 3.78\epsilon_0$).

strip, t/b, as a function of ratio $2a/b$ (width and height of the shielding) and is represented by the solid line in Fig. 8. Corresponding results obtained by the Green's function method [3] are denoted by the dashed line; good agreement between the two sets of results is evident. It is found that the influence of the side walls on the characteristic impedance is negligible when the walls are sufficiently removed from the strip, $2a/b > 5$.

For this example, the results obtained by using the singular and the infinite elements are compared with those derived by using only the ordinary elements. For the configuration in Fig. 7, for $2a/b = 2$, the lower and upper bounds of the characteristic impedance are 52.85 Ω and 55.20 Ω, respectively, when only the first-order ordinary elements are used and the mesh size N is 208 nodes. The inclusion of singular elements causes the bounds to come closer together, and the new values are found to be 53.47 Ω and 54.67 Ω. Even with ordinary elements, the gap between the lower and upper bounds can be narrowed by refining the mesh in the vicinity of the strip. However, in order to achieve accuracies comparable to those obtained with singular elements ($Z_{cl} = 53.40$ Ω and $Z_{cu} = 54.60$ Ω), the number of nodes has to be increased substantially, to 548. Thus, we observe that the use of singular elements results in a significant reduction in the number of nodes.

Likewise, if the same mesh with 208 nodes is used in the open-region geometry in conjunction with the infinite elements, the characteristic impedance is found to be $Z_c = 56.95$ Ω, which is close to that obtained (see Fig. 8) by placing the side walls sufficiently far from the center strip, say, by choosing $2a/b = 10$.

The next example is an inverted microstrip whose generic cross section [17], [19] is shown in Fig. 9. Calculated results for the characteristic impedance as a function of aspect ratio $2w/h$, denoted by the solid line, are compared with the numerical results obtained via the boundary element [BEM] method [19], shown by the dashed line in Fig. 10. Good agreement, within 5 percent, is obtained. Data for $\sqrt{\epsilon_{\text{eff}}}$ of the line as a function of aspect ratio $2w/h$ are presented in Fig. 11. Finite-element results are denoted by solid lines and BEM results by dashed lines. The measured points shown in the same figure were obtained via time-domain reflectometer measurements [29]. It can be noted that FEM results are closer to the experimental results than the BEM data. For the same example, attenuation constants due to conductor α_c and dielectric α_d losses

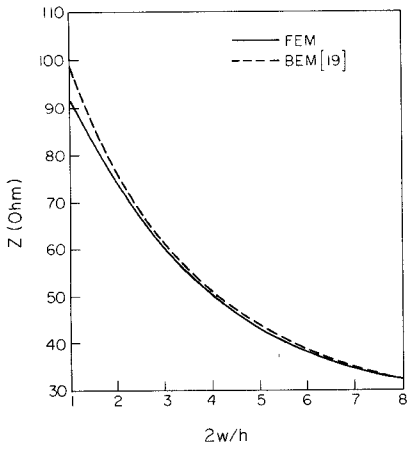

Fig. 10. Characteristic impedance Z of shielded inverted microstrip line versus shape ratio $2w/h$.

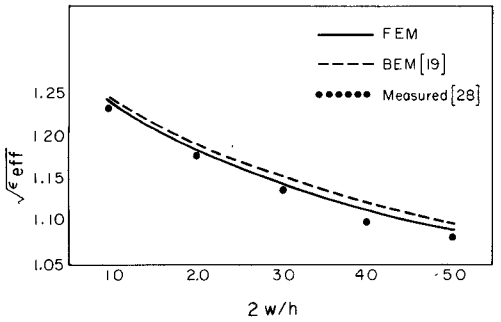

Fig. 11. $\sqrt{\epsilon_{eff}}$ of shielded inverted microstrip line versus shape ratio $2w/h$.

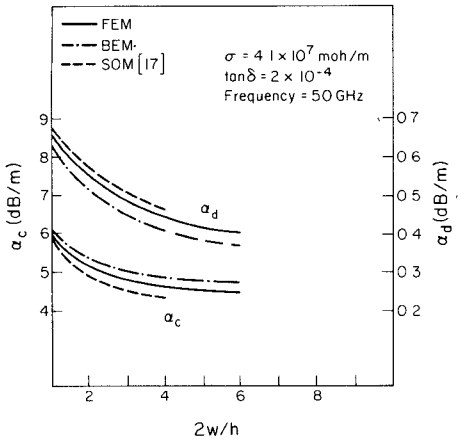

Fig. 12. Dielectric and conductor losses of shielded inverted microstrip line versus shape ratio $2w/h$.

are calculated as functions of aspect ratio $2w/h$ and shown in Fig. 12 as solid curves. These data are compared with BEM [19] and spectral-domain method [17] results, shown in the same figure, and very good agreement is found.

It should be pointed out that the accuracy of the calculation, especially of the loss calculations, can be significantly enhanced via the use of singular elements. The odd and even modes propagating on coupled lines can be treated by the same finite-element procedure. Some of the results for coupled lines are presented in [30].

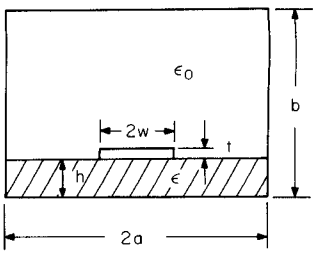

Fig. 13. Shielded microstrip line ($2a = 480$ mil; $b = 200$ mil; $h = 30$ mil; $2w = 93$ mil; $t = 0.8$ mil; $\epsilon = 2.2\epsilon_0$; $\tan\delta = 9\times10^{-4}$; $\rho = 1.7\times10^{-8}$ $\Omega - m$; $l = 2.97$ in).

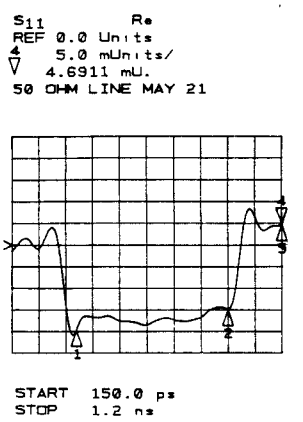

Fig. 14. Time-domain measured results.

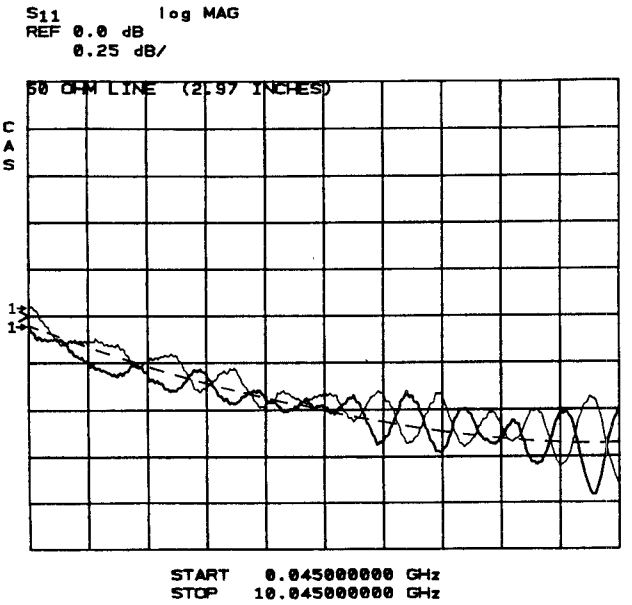

Fig. 15. Frequency-domain measured and calculated results of S_{11} parameter.
___: open-circuit measured results.
___: short-circuit measured results.
___: calculated values.

In order to verify the accuracy of the finite-element procedures, the characteristic impedance and losses of a shielded microstrip line have been measured. The experiment has been done on the line whose cross section and dimensions are shown in Fig. 13. By using a HP 8510 Network Analyzer, time-domain reflectometer measurements of characteristic impedance (Fig. 14) and

frequency-domain measurements of the S_{11} parameter of open- and short-circuited lines (Fig. 15) have been made. The measured value of characteristic impedance is 48 Ω, while the calculated value is 48.1 Ω. Excellent agreement between measured and calculated values of the S_{11} parameter of the line is found.

IV. Conclusions

In this study, a finite-element procedure for quasi-TEM analysis of microwave transmission lines is presented. The method is capable of handling microwave transmission lines with rather arbitrary configurations. Both first- and high-order triangular elements are employed. In the case of open-region problems (conductors over one or between two parallel ground planes) and edge singularity problems, the accuracy and efficiency of the method are enhanced via the use of infinite and singular elements. By solving both the original and the corresponding dual problem, the lower and upper bounds of the capacitance and the characteristic impedance are found. For the solution of finite-element linear equations, the band or the envelope matrix method (with reverse Cuthill–McKee reordering) is used for smaller systems and the incomplete Cholesky conjugate gradient method for large systems.

Computer software for semiautomatic mesh generation as well as for calculation of capacitance per unit length, effective permittivity, characteristic impedance, and attenuation due to conductor and dielectric losses has been developed.

Results obtained for various types of microwave transmission lines are in very good agreement with available theoretical and experimental data.

The method presented is both versatile and accurate. It can be readily extended to the lines with anisotropic media. Similar 3-D finite-element analysis would be a powerful tool for the calculation and design of connectors or lines with discontinuities. In future work, the authors plan to extend the FEM procedure to a full-wave analysis of microwave transmission lines.

Acknowledgment

The authors wish to thank B. M. Halpern of the Electrical and Computer Engineering Department of the University of Illinois for providing helpful assistance with the experimental part of this work.

References

[1] P. Silvester, "TEM wave properties of microstrip transmission lines," *Proc. Inst. Elec. Eng.*, vol. 115, pp. 43–48, Jan. 1968.

[2] T. G. Bryant and T. A. Weiss, "Parameters of microstrip transmission lines and of coupled pairs of microstrip lines," *IEEE Trans. Microwave Theory Tech.*, vol. MTT-16, pp. 1021–1027, Dec. 1968.

[3] E. Yamashita and K. Atsuki, "Analysis of thick-strip transmission lines," *IEEE Trans. Microwave Theory Tech.*, vol. MTT-19, pp. 120–122, Jan. 1971.

[4] R. Crampagne, M. Ahmadpanah, and T. Guirand, "A simple method for determining the Green's function for a large class of MIC lines having multilayered dielectric structures," *IEEE Trans. Microwave Theory Tech.*, vol. MTT-26, pp. 82–87, Feb. 1978.

[5] C. Wei, R. Harrington, L. Mautz, and T. Sarkar, "Multiconductor lines in multilayered dielectric media," *IEEE Trans. Microwave Theory Tech.*, vol. MTT-32, pp. 439–449, Apr. 1984.

[6] R. Mittra and C. Chan, "Iterative approaches to the solution of electromagnetic boundary value problems," to be published in special issue of *Electromagnetics, 1985.*

[7] S. Cohn, "Characteristic impedances of broadside-coupled strip transmission lines," *IRE Trans. Microwave Theory Tech.*, vol. MTT-8, pp. 633–637, Nov. 1960.

[8] T. Chen, "Determination of the capacitance, inductance, and characteristic impedance of rectangular lines," *IRE Trans. Microwave Theory Tech.*, vol. MTT-8, pp. 510–519, Sept. 1960.

[9] H. A. Wheeler, "Transmission-line properties of parallel strips separated by a dielectric sheet," *IEEE Trans. Microwave Theory Tech.*, vol. MTT-13, pp. 172–185, Mar. 1965.

[10] E. Yamashita and R. Mittra, "Variational method for the analysis of microstrip lines," *IEEE Trans. Microwave Theory Tech.*, vol. MTT-16, pp. 251–256, Apr. 1968.

[11] S. K. Koul and B. Bhat, "Generalized analysis of microstrip-like transmission lines and coplanar strips with anisotropic substrates for MIC, electrooptic modulator, and SAW application," *IEEE Trans. Microwave Theory Tech.*, vol. MTT-31, pp. 1051–1058, Dec. 1983.

[12] R. Mittra and T. Itoh, "Charge and potential distributions in shielded striplines," *IEEE Trans. Microwave Theory Tech.*, vol. MTT-18, pp. 149–156, Mar. 1970.

[13] A. El-Sherbiny, "Exact analysis of shielded microstrip lines and bilateral fin lines," *IEEE Trans. Microwave Theory Tech.*, vol. MTT-29, pp. 669–675, July 1981.

[14] A. Farrar and A. T. Adams, "Computation of propagation constants for the fundamental and higher order modes in microstrip," *IEEE Trans. Microwave Theory Tech.*, vol. MTT-24, pp. 456–460, July 1976.

[15] T. Itoh and A. S. Herbert, "A generalized spectral domain analysis for coupled suspended microstriplines with tuning septums," *IEEE Trans. Microwave Theory Tech.*, vol. MTT-26, pp. 820–826, Oct. 1978.

[16] T. Itoh, "Generalized spectral domain method for multiconductor printed lines and its application to tunable suspended microstrips," *IEEE Trans. Microwave Theory Tech.*, vol. MTT-26, pp. 983–987, Dec. 1978.

[17] D. M. Syahkal and J. B. Davies, "Accurate solution of microstrip and coplanar structures for dispersion and for dielectric conductor losses," *IEEE Trans. Microwave Theory Tech.*, vol. MTT-27, pp. 694–699, July 1979.

[18] R. F. Harrington *et al.*, "Computation of Laplacian potentials by an equivalent source method," *Proc. Inst. Elec. Eng.*, vol. 116, no. 10, pp. 1715–1720, Oct. 1969.

[19] B. E. Spielman, "Dissipation loss effects in isolated and coupled transmission lines," *IEEE Trans. Microwave Theory Tech.*, vol. MTT-25, pp. 648–655, Aug. 1977.

[20] P. Daly, "Hybrid-mode analysis of microstrip by finite-element method," *IEEE Trans. Microwave Theory Tech.*, vol. MTT-19, pp. 19–25, Jan. 1971.

[21] P. Silvester, "High-order polynomial triangular finite elements for potential problems," *Int. J. Eng. Sci.*, vol. 7, pp. 849–861, 1969.

[22] P. Tracey and T. Cook, "Analysis of power type singularities using finite elements," *Int. J. Num. Methods Eng.*, vol. 11, pp. 1225–1233, 1977.

[23] J. Meixner, "The behaviour of electromagnetic fields at edges," New York University, New York, NY, Inst. Math. Sci. Res. Rep. EM-72, Dec. 1954.

[24] F. Medina and R. Taylor, "Finite element techniques for problems of unbounded domains," *Int. J. Num. Methods Eng.*, vol. 19, pp. 1209–1226, 1983.

[25] C. T. Carson and G. K. Combrell, "Upper and lower bounds on the characteristic impedance of TEM mode transmission lines," *IEEE Trans. Microwave Theory Tech.*, vol. MTT-14, pp. 497–498, Oct. 1966.

[26] J. D. Jackson, *Classical Electrodynamics*. New York: Wiley, 1966, 236–240.

[27] Z. Pantić and R. Mittra, "Finite element matrices for loss calculation in quasi-TEM analysis of transmission lines," to be published.

[28] O. Axelsson and V. A. Barker, *Finite Element Solution of Boundary Value Problems — Theory and Computation*. New York: Academic Press, 1984.

[29] M. V. Schneider, "Microstrip lines for microwave integrated circuits," *BSTJ*, vol. 48, no. 5, pp. 1421–1444, May–June 1961.

[30] Z. Pantić and R. Mittra, "Quasi-TEM analysis of isolated and coupled microwave transmission lines by the finite element method," presented at URSI Conference (Vancouver), June 1985.

✠

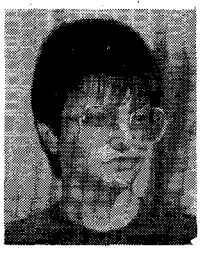

Zorica Pantić was born in Belgrade, Yugoslavia. She received the B.Sc., M.Sc., and D.Sc. degrees from the University of Niš in 1975, 1978, and 1982, respectively.

In 1976, she joined the Department of Electronic Engineering at the University of Niš as a Teaching Assistant in electromagnetics. In 1986, she was appointed Docent in antenna theory and propagation and microwaves at the same department. From August 1984 to August 1985, she was with the Department of Electrical and Computer Engineering at the University of Illinois, Urbana-Champaign, as a Visiting Fulbright Scholar in the Electromagnetic Communication Laboratory. Since August 1985, she has been a Visiting Research Associate with the same department. Her research interests are in the areas of analytical and computer-aided electromagnetics, microwave passive components, electromagnetic scattering and diffraction, and antennas.

✠

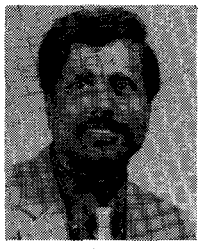

Raj Mittra (S'54–M'57–SM'69–F'71) is Director of the Electromagnetic Communication Laboratory of the Electrical and Computer Engineering Department and Research Professor of the Coordinated Science Laboratory at the University of Illinois. He is a past president of the Antennas and Propagation Society of the IEEE. He serves as a consultant to several industrial and governmental organizations in the United States and abroad.

His professional interests include the areas of analytical and computer-aided electromagnetics, high-speed digital circuits, radar scattering, satellite antennas, microwave and millimeter-wave integrated circuits, frequency selective surfaces, EMP and EMC analysis, and the interaction of electromagnetic waves with biological media.